A SUPER-RESOLUTION MICROSCOPY WITH STANDING EVANESCENT LIGHT AND IMAGE RECONSTRUCTION METHOD

Hiroaki Nishioka[1], *Satoru Takahashi*[1] *Kiyoshi Takamasu*[1]

[1]Department of Precision Engineering, The University of Tokyo, Tokyo, Japan, nishioka@nano.pe.u-tokyo.ac.jp

Abstract: We propose a super-resolution microscopy that employs standing evanescent light illumination and image reconstruction method with successive approximation.

Samples are illuminated with standing evanescent light, which is formed and shifted into different positions on the interface of total internal reflection (TIR). Scattering light emitted from the illuminated samples is detected through far-field imaging optics. We assume two hypotheses of linearity and incoherence about the scattering light. Then we reconstruct the sample distribution from scattering images and standing evanescent light intensity with successive approximation.

We examined this microscopy with one-dimensional computer simulation and demonstrated that super resolution over the diffraction limit is achievable. The resolution power improves with shorter peak-to-peak distance of standing evanescent light and more cycles of the reconstruction calculation. As a possible resolution, two dot samples separated by 50 nm were resolved when the wavelength is 633 nm and the diffraction limit is 594 nm.

With two-dimensional computer simulation, we were also able to resolve random dot samples in super resolution by using longitudinal and transversal standing evanescent light.

Keywords: super resolution, standing evanescent light, image reconstruction method.

1. INTRODUCTION

Nanometrology is one of the fundamental technologies that support the recent development of nanotechnology. Many types of microscopy have been developed to improve performance in resolution, throughput, noninvasiveness, etc.

Electron microscopy such as SEM and TEM achieves powerful high resolution, but the electron beam gives damage to samples and the restricted condition involving vacuum environment decreases its application and throughput. As for scanning probe microscopes (SPM) such as STM[1] and AFM[2], the scanning probe mechanism enables atomic resolution but suffers from low throughput because of the necessity of contact with samples.

Optical microscopy is a superior metrology to solve the disadvantages mentioned above. Because light has intrinsic characteristics of low energy and spatial transmission, no damage is given to samples and high throughput is achievable by remote imaging.

But the major limitation of optical microscopy is the diffraction limit in resolution, which is about half the wavelength[3]. Various types of optical microscopy have been developed so far to overcome the diffraction limit, such as confocal microscopy[4,5], SNOM[6,7] and TIR fluorescence microscopy[8,9]. In this paper, we propose a novel type of TIR microscopy that employs combined use of standing evanescent light and image reconstruction. This microscopy can achieve super resolution of several ten nanometers over the diffraction limit. High throughput is also achievable because a whole field of the TIR interface is simultaneously measurable. This proposed microscopy also has a noninvasive benefit of optical microscopy.

Now in the downsizing scale and accelerating pace in research and development in nanotechnology, there is a need for a microscopy that combines high resolution, high throughput and noninvasiveness. The proposed microscopy has a well-balanced advantage in these features.

This super-resolution microscopy is widely applicable to any kind of transparent surfaces with any wavelengths of light, such as cover glass surfaces with visible light in biotechnology and silicon wafer surfaces with infrared light in semiconductors.

2. PRINCIPLE OF THE SUPER-RESOLUTION MICROSCOPY

2.1. Standing evanescent light illumination and shift

Standing evanescent light is formed on the interface of total internal reflection by a superposition of an incident light and a reflecting light (Fig.1). Illuminate samples are confined within several hundred nanometers from the TIR interface because the intensity of evanescent light decreases exponentially in a vertical direction. The standing evanescent light has high-frequency modulation in a lateral direction, whose peak-to-peak distance is about half the wavelength (several hundred nanometers).

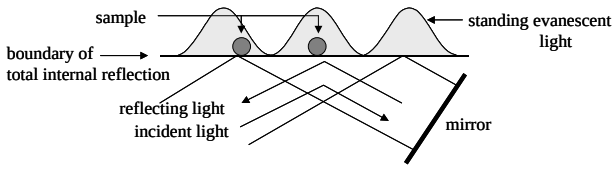

Fig. 1. Standing evanescent light illumination

We can shift the position of standing evanescent light by several nanometers by shifting the reflecting mirror with a piezoelectric actuator (Fig.2). The illuminated samples emit scattering light and we can give change to its intensity with the standing evanescent light shift.

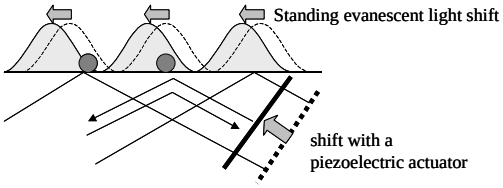

Fig. 2. Standing evanescent light shift

2.2. Optical imaging of scattering light

Scattering light from the TIR interface is magnified and detected through far-field imaging optics. We assume two hypotheses about scattering light to describe this optical imaging.

First hypothesis is linearity between a scattering light intensity I_i and an illumination light intensity E_i (Fig.3). We assume that a dot sample emits scattering light whose intensity I_i is proportional to the illumination intensity E_i.

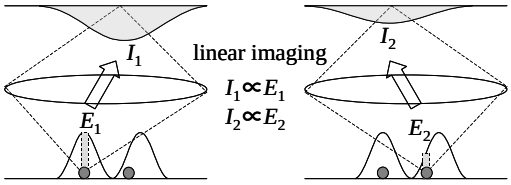

Fig. 3. Hypothesis of linearity of scattering light

This is written as the following equation (1), where a_i is a proportional constant. a_i is inherent in the optical property of the dot sample.

$$I_i = a_i \cdot E_i \tag{1}$$

Then we define a_i as a physical quantity of a dot sample, which is determined by $a_i=I_i/E_i$ from equation (1). This represents a scattering efficiency of a dot sample and we can describe an arbitrary sample distribution by scattering efficiency (Fig.4). Here scattering efficiency $a(x)$ is defined between 0 and 1 for simplification. For example, if a sample distribution is discrete, we can set $a(x)=1$ at the positions of dot samples, and $a(x)=0$ in the other space. If a sample distribution is continuous, we can set high scattering efficiency in the high-density sample areas and low in the diluted areas. No scattering light is emitted from where $a(x)=0$, which is understandable from the equation (1).

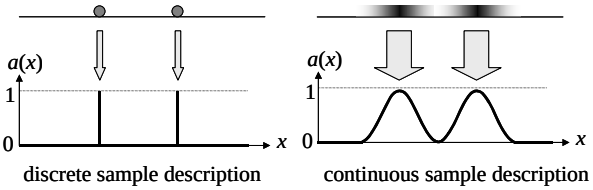

Fig. 4. Sample description by scattering efficiency

Second hypothesis is incoherence of scattering light. We assume scattering light from a whole field of the TIR interface is emitted in the incoherent condition. If a sample distribution is discrete, the final scattering image is determined by a simple summation of each image from each dot sample (Fig.5).

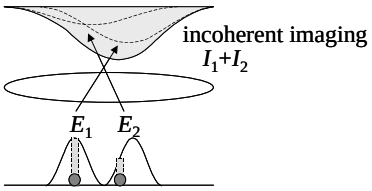

Fig. 5. Hypothesis of incoherence of scattering light

With these hypotheses, we can now describe the optical imaging phenomenon in a general case. Scattering image $I(x)$ is determined from sample distribution $a(x)$ and illumination intensity $E(x)$ by the following equation (2). PSF is a point-spread function of the imaging optics, which represents the airy disk image by the diffraction.

$$I(x) = PSF(x) \otimes (a(x) \cdot E(x)) \tag{2}$$

The equation (2) enables us to simulate scattering image $I(x)$ from $a(x)$ and $E(x)$. We can change the scattering image $I(x)$ by shifting the standing evanescent light intensity $E(x)$ into different positions. This is illustrated in Fig.6 with an example of two dot samples.

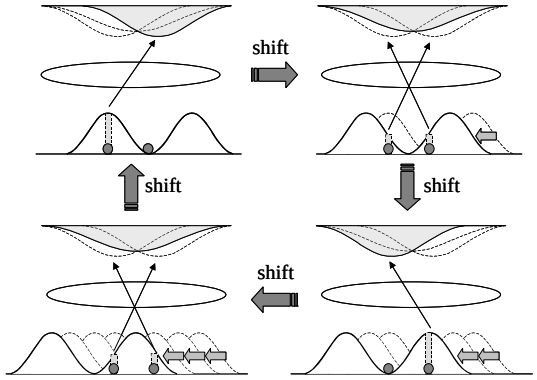

Fig. 6. Change of scattering image caused by illumination shift

This far-field optical imaging is dominated by the diffraction limit. Because PSF(x) acts as a low pass filter in the equation (2), high-frequency information of sample distribution $a(x)$ is lost in scattering image $I(x)$ through the imaging optics. But the equation (2) enables us to reconstruct sample distribution $a(x)$ from $I(x)$ and $E(x)$. When both $I(x)$ and $E(x)$ are known, we can reconstruct $a(x)$ with successive approximation. Thus we expect to achieve super resolution over the diffraction limit. This is explained in the following image reconstruction method.

2.3. Image reconstruction method

The flow chart of image reconstruction method is shown in Fig.7. In order to reconstruct sample distribution, an assumed sample distribution is successively approximated by use of the equation (2).

We set two integer parameters of *SHIFT* and *LOOP*. We shift standing evanescent light m times by a constant distance within its peak-to-peak distance. The parameter *SHIFT* determines which position of the standing evanescent light to select for illumination, and this parameter circulates between 1 and m during the

reconstruction calculation. The parameter *LOOP* counts how many times the parameter *SHIFT* circulated up to *m* until the end of the repeated calculation.

We begin the flow chart with assuming initial constant sample distribution because real sample distribution $a_0(x)$ is unknown. This is input into assumed sample distribution $a(x)$. Then we select illumination intensity $E(x)$ from shifted standing evanescent lights in accordance with the parameter *SHIFT*, and illuminate both the real sample and the assumed sample. This illumination and following optical imaging yield observed scattering image $I_0(x)$ which is obtained experimentally and assumed scattering image $I(x)$ which is calculated based on the equation (2).

$$I(x) = PSF(x) \otimes (a(x) \cdot E(x)) \tag{2}$$

Here we compare the assumed scattering image with the observed scattering image by evaluating $I_0(x)/I(x)$ as observed/assumed error. Because we are able to modify $I(x)$ by reconstructing $a(x)$ in the equation (2), we approximate the assumed sample distribution $a(x)$ into a reconstructed sample distribution so that the error $I_0(x)/I(x)$ in the scattering images should be minimized.

We perform this reconstruction approximation for every position of the standing evanescent light while the parameter *SHIFT* circulates from 1 to *m*. This cycle of *m* times calculations is counted by the parameter *LOOP*, and successively repeated as the parameter *LOOP* increases. When the parameter *LOOP* reaches *n*, we terminate reconstruction and acquire the final reconstructed sample distribution as a result.

The nanometer-scale shifts of standing evanescent light that is modulated in about half-wavelength scale include high-frequency spatial information and this causes change to scattering images. We expect to achieve super resolution by feeding back the errors in scattering images into sample distribution and reconstructing the sample distribution with successive approximation.

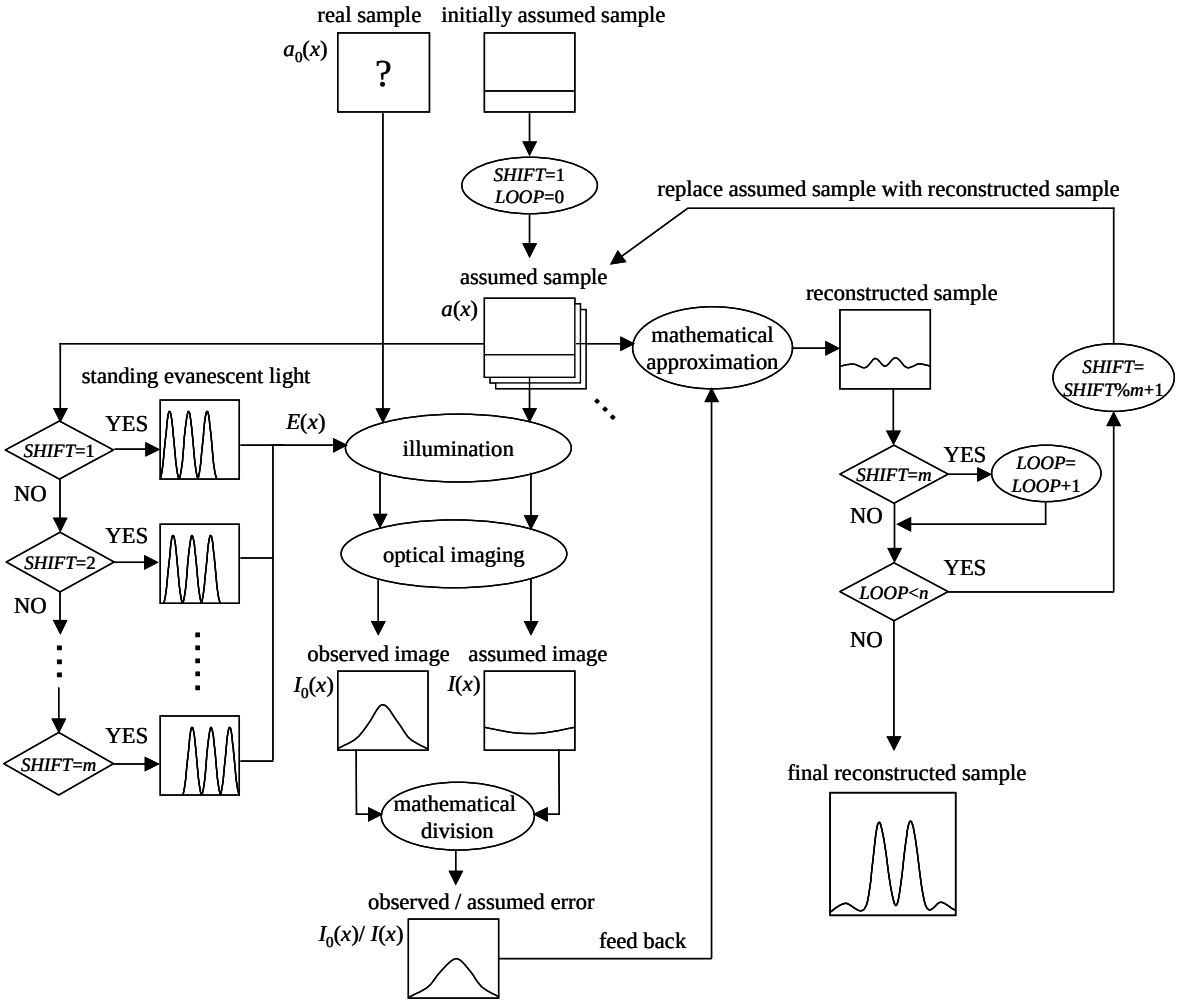

Fig. 7. Flow chart of the reconstruction calculation

3. VERIFICATION OF THE SUPER-RESOLUTION MICROSCOPY WITH ONE-DIMENSIONAL COMPUTER SIMULATION

We verified the proposed super-resolution microscopy in one-dimensional computer simulation. The basic simulation conditions are shown in Table.1.

Table.1. Simulation conditions

Items	Value
Wavelength of light	633nm
Higher refractive index of medium (glass)	1.53
Lower refractive index of medium (air)	1.0
Incident angle of illumination light	75 deg.
Peak-to-peak distance of standing evanescent light	214nm
m (maximum of the parameter *SHIFT*)	15
Numerical aperture of imaging optics	0.65
Diffraction limit	594nm

3.1. Verification of sample reconstruction

First we verified sample reconstruction by the proposed microscopy near the condition of the diffraction limit.

We set two dot samples separated by 600 nm and described sample distribution $a_0(x)$ with scattering efficiency as in Fig.8 (a). If this sample distribution is observed by conventional optical microscopy, the scattering image becomes vague as in Fig.8 (b) by the diffraction limit of the imaging optics.

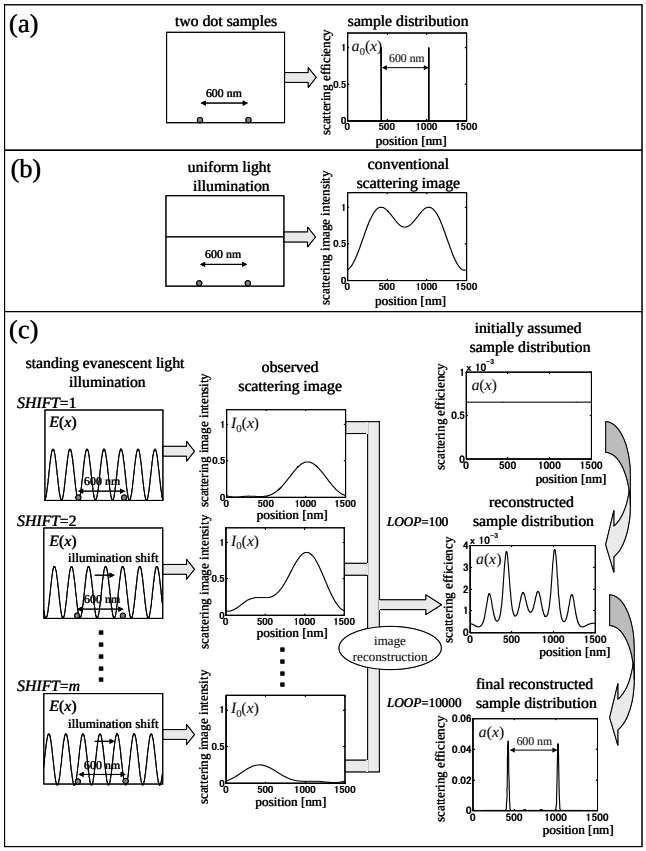

Fig. 8. Super-resolution simulation near the diffraction limit
(a) description of samples (b) conventional optical imaging
(c) proposed super-resolution microscopy

Then we applied the proposed microscopy to this sample distribution. The result is shown in Fig.8 (c).

As standing evanescent light is shifted rightward with the parameter SHIFT and two dot samples are dynamically illuminated, observed scattering image $I_0(x)$ gradually changes. Although these observed scattering images are usually obtained experimentally, we calculated them based on the following equation (3) in this computer simulation.

$$I_0(x) = PSF(x) \otimes (a_0(x) \cdot E(x)) \tag{3}$$

Then we applied the image reconstruction method with these $I_0(x)$ to the initially assumed constant sample distribution. The flow chart in Fig.7 successively yielded reconstructed sample distributions $a(x)$. Two results are shown when *LOOP*=100,10000. It shows that the reconstructed sample distribution $a(x)$ gradually approaches the real sample distribution $a_0(x)$. Finally we could resolve two dot samples with clear separation when *LOOP*=10000.

Thus we demonstrated that sample reconstruction is possible by the proposed microscopy near the condition of the diffraction limit.

3.2. Super resolution over the diffraction limit

Then we examined the feasibility of super resolution of the proposed microscopy with an example of two dot samples separated by 200 nm and 100 nm.

The result is shown in Fig.9. The upper and lower row is the case of 200 nm and 100 nm, respectively. The left figures are the real sample distributions. The middle figures are scattering images observed by conventional optical microscopy. And the right figures are the reconstructed sample distributions by the proposed microscopy.

The conventional scattering images are no longer resolvable because the separations are smaller than the diffraction limit of 594 nm. But we could resolve 200 nm with clear separation and 100 nm with the Rayleigh criterion by means of the proposed microscopy.

Thus we demonstrated that super resolution over the diffraction limit is achievable by the proposed microscopy. In particular, resolutions of 200 nm and 100 nm were achieved when the wavelength is 633 nm and the diffraction limit is 594 nm

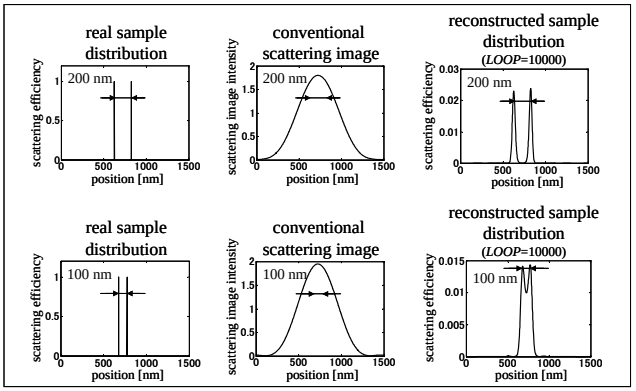

Fig. 9. Super-resolution simulation over the diffraction limit

3.3. Characteristics of super resolution

We analyzed super-resolution characteristics of the proposed microscopy. We examined resolution power in relations to peak-to-to distance of standing evanescent light and cycles of the reconstruction calculation.

We define resolution power from reconstructed sample scattering efficiency by the following equation (4) and Fig.10.

$$resolution \quad power = (h_1 + h_2)/2l \tag{4}$$

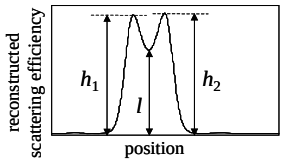

Fig. 10. Definition of resolution power

3.3.1. Peak-to-peak distance of standing evanescent light

We can change peak-to-peak distance of standing evanescent with different incident angles of illumination light in the range of the TIR condition.

In order to examine the relation between resolution power and peak-to-peak distance of standing evanescent light, two dot samples with 100 nm separation were reconstructed with different incident angles until *LOOP*=10000. Then we plotted resolution power against peak-to-peak distance in Fig.11.

The result shows that the resolution power of the proposed microscopy improves with shorter peak-to-peak distance of standing evanescent light. In this condition, resolution over the Rayleigh criterion is achievable when peak-to-peak distance is less than 220 nm, that is, when the incident angle is more than 70 degrees. But there is a limitation of maximum of 90 degrees in the incident angle, which corresponds to 207 nm of peak-to-peak distance.

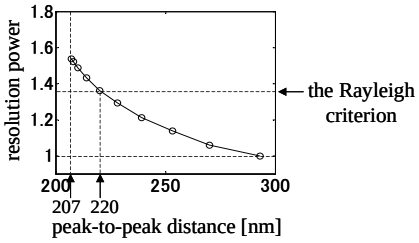

Fig. 11. Resolution power against peak-to-peak distance of standing evanescent light

3.3.2.Cycles of the reconstruction calculation

We examined the relation between the resolution power of the proposed microscopy and cycles of the reconstruction calculation.

Two dot samples with 100 nm separation were reconstructed with different cycles of the reconstruction calculation. We plotted resolution power against cycles of the reconstruction calculation in Fig.12.

The result shows that the resolution power of the proposed microscopy improves with more cycles of the reconstruction calculation. In this condition, resolution over the Rayleigh criterion is achievable when cycles are more than 10^4.

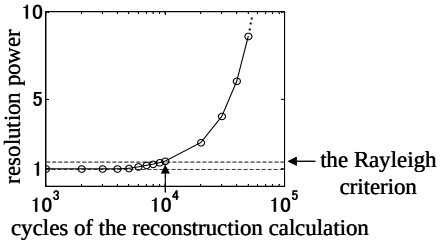

Fig. 12. Resolution power against cycles of the reconstruction calculation

3.3.3. Possible resolution

As shown in Fig.11 and Fig.12, we can improve the resolution power by decreasing peak-to-peak distance of standing evanescent light and by increasing cycles of the reconstruction calculation.

As the scale becomes smaller, the size of dot samples would not be negligible in comparison with the separation distance. When the separation becomes about the same scale as the sample size, two samples would be no longer independent because the near-field electromagnetic field from one sample affects that of the other. But as long as samples can be considered independent of each other, this super-resolution microscopy is would be applicable.

Then we examined a possible resolution of the proposed microscopy with an example of two dot samples separated by 50 nm. As for simulation conditions, we set 208 nm and 214 nm for peak-to-peak distance of standing evanescent light and 10^6 and 10^4 for cycles of the reconstruction calculation, respectively. Other simulation conditions are the same as in Table.1. The results are shown in Fig.13.

Resolution improvement has been confirmed in Fig. (a) in comparison with Fig.13 (b) and we could successfully resolve 50 nm separation satisfying the Rayleigh criterion.

Thus we demonstrated that 50 nm is a possible resolution of the proposed microscopy when the wavelength is 633 nm and the diffraction limit is 594 nm.

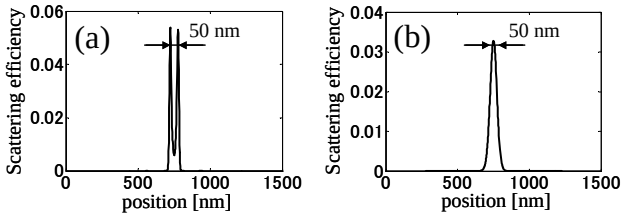

Fig. 13. Reconstructed sample distribution with 50 nm separation (a) with 10^6 cycles of reconstruction calculation and 208 nm of peak-to-peak distance (b) with 10^4 cycles of reconstruction calculation and 214 nm of peak-to-peak distance

4. TWO-DIMENSIONAL SUPER RESOLUTION IN COMPUTER SIMULATION

We also examined the feasibility of two-dimensional super resolution of the proposed microscopy with an example of random dot samples on the TIR interface. The simulation conditions are the same as in Table.1.

We used longitudinal and transversal standing evanescent lights for illumination and shifted them in parallel directions with their spatial modulations. This is illustrated in Fig.14.

The result is shown in Fig.15 in comparison with normal scattering image observed by conventional optical microscopy. The upper figure is the sample distribution. The middle figure is the conventional scattering image, where all dot samples are vague and close dot samples are already merged. Here the resolution is limited by the diffraction limit of 594 nm.

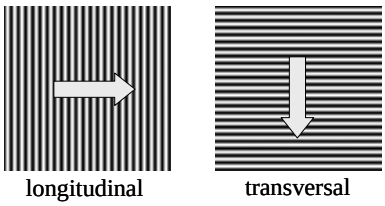

Fig. 14. Longitudinal and transversal standing evanescent light illumination and shift

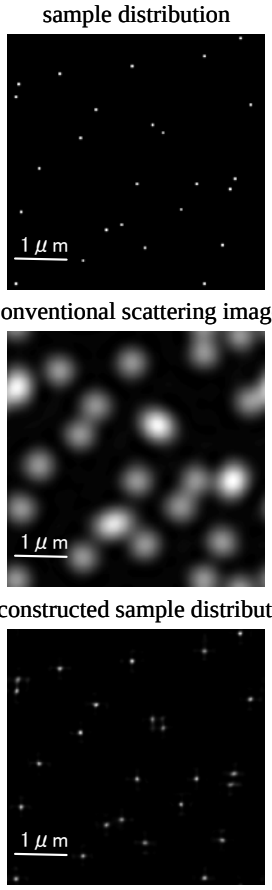

Fig. 15. Two-dimensional super resolution in computer simulation

On the contrary, the lower figure is the reconstructed sample distribution by the proposed microscopy, where all dot samples are sharpened and close dot samples are resolved separately. In particular, 200 - 300 nm separations were successfully resolved.

Thus it was demonstrated that two-dimensional super resolution is also achievable by the proposed microscopy.

5. CONCLUSION

We proposed a super-resolution microscopy that employs standing evanescent light and image reconstruction method with successive approximation.

Standing evanescent light is formed and shifted into different positions on the TIR interface, and scattering light from samples is detected through far-field imaging optics. We assumed two hypotheses of linearity and incoherence about the scattering light, and described the imaging phenomenon with a point-spread function. Then we reconstructed the sample distribution from scattering images and standing evanescent light intensity with successive approximation.

We examined the feasibility of the proposed microscopy. In one-dimensional computer simulation, we demonstrated that sample reconstruction is possible and that super resolution over the diffraction limit is achievable. The resolution power improves with shorter peak-to-peak distance of standing evanescent light and more cycles of the reconstruction calculation. We demonstrated that 50 nm is a possible resolution when the wavelength is 633 nm and the diffraction limit is 594 nm.

In two-dimensional computer simulation, we successfully resolved random dot samples in super resolution by using longitudinal and transversal standing evanescent lights.

REFERENCES

[1] G. Binning and H. Rohrer, “Scanning tunneling microscopy”, IBM J. Res. Dev. 30, 355 (1986)

[2] G. Binning, C.F. Quante and C. Gerber, “Atomic force microscope”, Phys. Rev. Lett. 12, 930-933 (1986)

[3] M. Born and E. Wolf (eds.), “Principles of Optics”, Pergamon Press (1980)

[4] T. Wilson and C. Sheppard, “Theory and Practice of Scanning Optical Microscopy”, Academic Press (1984)

[5] T. Wilson, “Confocal Microscopy”, Academic Press (1990)

[6] U. Durig, D. W. Pohl and F. Rohner, J. Appl. Phys. 59, 3318 (1986)

[7] E. Betzig, M. Isacson and A.Lewis, Appl. Phys. Lett. 51, 2088 (1987)

[8] Axelrod D., “Total internal reflection fluorescence microscopy”, Method in Cell Biology, 30, 245-270 (1989)

[9] G. Cragg and P. T. C. So, “Standing-wave total internal reflection”, Opt. Lett. 25, 46-48 (2000)